Plasmons-Enhanced Minority-Carrier Injection as a Measure of Potential Fluctuations in Heavily Doped Silicon

Ming-Jer Chen, *Senior Member, IEEE*, Chuan-Li Chen, Shang-Hsun Hsieh, and Li-Ming Chang

***Abstract*— Well-known apparent electrical silicon bandgap narrowing in a heavily doped region of a bipolar transistor is observed by means of an enhanced minority-carrier injection experiment. In the region of interest, plasmons-induced potential fluctuations are existent in nature and hence constitute the origin of apparent bandgap narrowing. In this letter, we extract the underlying potential fluctuations directly from the enhanced minority-carrier injection experiment published in the literature. The core of the extraction lies in a combination of the two existing theoretical frameworks. First, the Gaussian distribution can serve as a good approximation of potential fluctuations. Second, no change can be made in the real bandgap between fluctuating conduction- and valence-band edges. Extracted potential fluctuations come from plasmons, as verified by our published temperature dependences of plasmons limited mobility in the inversion layer of MOSFETs as well as theoretical calculation results on bulk silicon. More importantly, this letter can deliver potential applications in the modeling and simulation area of nanoscale FETs (MOSFETs, FinFETs, and so forth) and bulk semiconductors.**

***Index Terms*— Bandgap narrowing, bipolar transistor, device physics, field-effect transistors (FETs), fluctuations, long-range Coulomb interactions, plasmons, transport.**

I. Introduction

FOR doped semiconductors, there are naturally many-body phenomena, such as the plasmons (e.g., quantized collective modes of interacting particles [1]) and potential fluctuations. Currently, at the device level, plasmons in the highly doped region are of increasing importance, particularly for FETs at the nanometer dimension [2]. The reason is that potential fluctuations caused by plasmons in the highly doped source and drain will significantly penetrate into the channel and thereby deteriorate the device performance via long-range collective Coulomb interactions [3]. Sophisticated device simulation tasks [3], [4] and a carefully-calibrated temperature dependent experiment [5] have separately corroborated this. Thus, it is highly desirable to experimentally determine the amount of plasmons induced potential fluctuations at the semiconductor level.

Manuscript received April 17, 2014; revised May 5, 2014, May 10, 2014, and May 13, 2014; accepted May 14, 2014. Date of publication June 9, 2014; date of current version June 24, 2014. This work was supported by the National Science Council of Taiwan under Contract NSC 101-2221-E-009-057-MY3. The review of this letter was arranged by Editor A. Ortiz-Conde.

The authors are with the Department of Electronics Engineering, Institute of Electronics, National Chiao Tung University, Hsinchu 300, Taiwan (e-mail: chenmj@faculty.nctu.edu.tw; recreation2266.ep97@g2.nctu.edu.tw; fantasytint@hotmail.com; chang7081@gmail.com).

Color versions of one or more of the figures in this letter are available online at http://ieeexplore.ieee.org.

Digital Object Identifier 10.1109/LED.2014.2325030

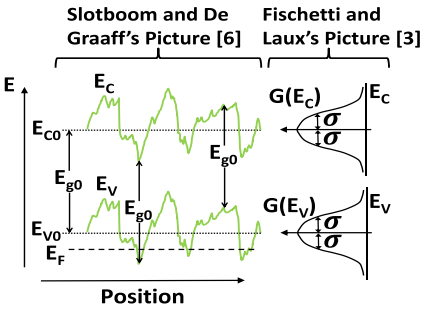

Fig. 1. Combined theoretical frameworks [3], [6] to deal with the potential fluctuations due to many-body effects in p-type semiconductor.

To achieve the goal, the two theoretical frameworks in the literature [3], [6] may be helpful. The first framework is associated with an enhanced *minority-carrier* injection experiment in the heavily doped region of a bipolar transistor [6]–[10]. In the experiment [6]–[10], the intrinsic concentration was found to increase with the doping concentration, hence leading to the well-known *apparent* electrical bandgap narrowing. Relative to other origins proposed (see [6] for the details), Slotboom and De Graaff [6] favored a physical picture, with no solid evidence at the time, that *long range impurity density fluctuations can cause potential fluctuations, which increase the averaged pn-product without a change in the band gap*. If one slightly changes "impurity" in this statement to "charge", then the resulting picture is exactly of plasmons [1] and hence serves as the first theoretical framework (other many-body effects will be discussed later). As schematically shown in Fig. 1, the same potential fluctuations occur both in the conduction- and valence-band edges while the bandgap remains intact and independent of the doping.

Potential fluctuations due to plasmons or other many-body effects essentially are spatially dependent and vary with time [1]. Fortunately, Fischetti and Laux [3] pointed out that such complicated behaviors can be well approximated by a position-averaged and time-averaged quantity, namely the Gaussian distribution. This constitutes the second framework, as shown in the figure.

So far, the second framework was applied [3] to the *conduction-band edge only* (in n-type silicon). Even both

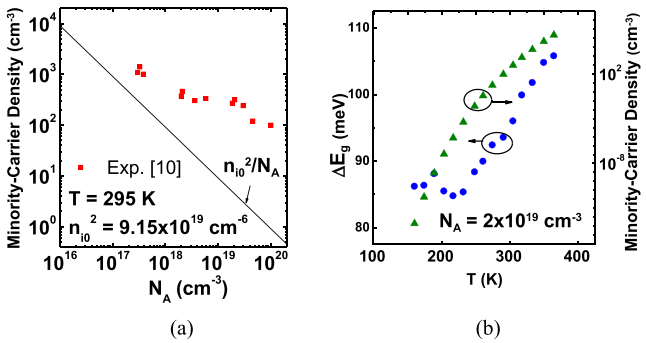

Fig. 2. Experimental data from the injection experiment [10] in terms of (a) the minority-carrier density versus doping concentration and (b) minority-carrier density and apparent electrical bandgap narrowing versus temperature.

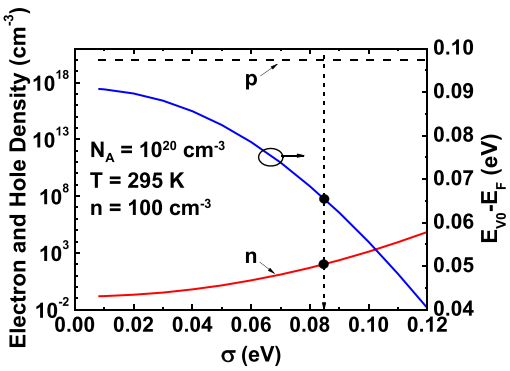

Fig. 3. Calculated electron density, hole density, and Fermi level as a function of the standard deviation of the Gaussian distribution for $N_A = 10^{20}$ cm^{-3} at 295 K. Corresponding experimental minority-carrier density of around 100 cm^{-3} [10] determines the underlying σ and E_F.

frameworks were not combined in such a way to *directly* extract potential fluctuations from the *increased minority-carrier density* in the aforementioned injection experiment. In this letter, we combine these two theoretical frameworks to make possible such a direct extraction of potential fluctuations due to plasmons. Potential applications are straightforwardly drawn.

II. Data and Equations

The minority-carrier injection experiment in p-type silicon conducted by Swirhun et al. [10] is quoted here, because the available data as plotted in Fig. 2 are quite complete. In the experiment [10], the majority-carrier density p was made to be equal to N_A; and the intrinsic concentration n_{i0} adopted the following empirical formula:

$$n_{io} = 3.563 \times 10^{16} \times T^{1.5} \exp(-6.98 \times 10^3 / T) \qquad (1)$$

It can be seen from Fig. 2(a) that the experimental minority-carrier density lies above a straight line with no bandgap narrowing. Such difference tends to increase with increasing doping concentration, meaning that the minority-carrier injection is enhanced. Values of apparent electrical bandgap narrowing ΔE_g in Fig. 2(b) were obtained from the experimental minority-carrier density n through the following equation [10]:

$$n = (n_{i0}^2 / N_A) \exp(\Delta E_g / k_B T). \qquad (2)$$

On the other hand, there are two equations that can be drawn from the theoretical frameworks in Fig. 1:

$$n = \int_{-\infty}^{\infty} \int_{E_C}^{\infty} DOS_C(E) f_{FD}(E) dE G(E_C) dE_C \qquad (3)$$

$$p = \int_{-\infty}^{\infty} \int_{-\infty}^{E_V} DOS_V(E)(1 - f_{FD}(E)) dE G(E_V) dE_V \qquad (4)$$

where DOS_C and DOS_V are the conduction and valence band densities of states (*DOS*), respectively; f_{FD} is the Fermi-Dirac distribution function; and G is the Gaussian distribution with the standard deviation σ (see Fig. 1). Corresponding electron and hole DOS effective masses of $m^*_{DOSc} = 1.182 m_0$ and $m^*_{DOSv} = 0.81 m_0$ [11], respectively, were used in this work. The band edge reference E_{C0} and E_{V0} are the mean of the Gaussian distribution in the fluctuating conduction- and valence-band edges, respectively. The bandgap E_{g0} of 1.08 eV at 295 K comes from (1). Eqs. (3) and (4) are coupled each other due to the common factor, the Fermi level E_F of the system. In the limiting case of $\sigma \to 0$, (3) and (4) exactly reduce to those of standard form [11].

III. Extraction Results and Discussion

Two remaining parameters need to be extracted for a given N_A: σ and E_F. To demonstrate the extraction process in detail, we fix N_A at 10^{20} cm^{-3} at 295 K. First, we adjust E_F to make the calculated majority-carrier density from (4) equal to N_A. Resulting E_F is plotted in Fig. 3 versus σ. Clearly, an increase in σ will make E_F move more upward and hence closer to the conduction-band edge. This is the physical origin of the observed minority-carrier injection enhancement. Next, we make the calculated minority-carrier density from (3) equal to the experimental value of around 100 cm^{-3} (see Fig. 2(a)). This leads to extracted σ of 85 meV and hence underlying E_F of 65 meV below E_{V0}, as depicted in Fig. 3. Meanwhile, $p \gg n$ and hence the charge neutrality, on the average, is satisfied. Note that if no experimental minority-carrier density acts as numerical constraints, σ and E_F will have infinite solutions. Similar extraction tasks were carried out for other temperatures and doping concentrations. Extracted potential fluctuations are given in Fig. 4. *Evidently, a decrease in temperature tends to weaken the plasmons and hence potential fluctuations.*

We present the two approaches to support plasmons as the origin of the extracted σ. The first approach is achieved through temperature-dependent measurements of plasmons limited mobility in the inversion layer of MOSFETs, as had been done in our previous works [5] and [13]. Temperature power law of corresponding mobility follows T^{-1} for surface plasmons in the polysilicon gate [13] and $T^{-0.7}$ for bulk plasmons in the source and drain [5]. To make the comparison possible, we employ a delta-type potential approximation [12] (that is, the mean relaxation time is inversely proportional to

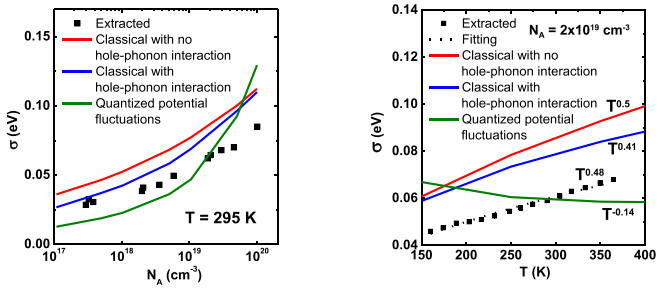

(a) (b)

Fig. 4. Extracted potential fluctuations plotted versus (a) doping concentration and (b) temperature. Also plotted are calculated classical and quantum potential fluctuations. Hole-phonon interaction is considered in the calculated classical potential fluctuations. Corresponding temperature power laws are added for comparison.

the square of σ). As a result, the power law of extracted $\sigma(T^{0.48})$ is transformed to that of corresponding mobility ($T^{-0.96}$). Strikingly, these power law exponents of mobilities are comparable each other.

The second approach goes to the two theoretical calculations: one of the quantized potential fluctuations [3]:

$$\sigma_{QPF} = \left(\frac{\hbar\omega_p q_c}{4\varepsilon_s \pi^2}\right)^{1/2} \times \sqrt{1+2n_p} \tag{5}$$

and one of the classical potential fluctuations [3]:

$$\sigma_{CL} = \left(1.451 \times \frac{3}{2\pi}\right)^{1/2} \times \frac{en^{2/3}}{\varepsilon_s \beta_s} \tag{6}$$

All parameters in these equations are known: the plasmon frequency ω_p, the cut-off wavevector q_c, the semiconductor permittivity ε_s, and the inverse of screening length β_s, with the n_p following the Bose-Einstein distribution. Calculated results are added to Fig. 4. It can be seen that only classical calculations can adequately reproduce data concerning both doping and temperature effects. Calculated temperature dependence from the quantum method is far from reality, whose interpretations will be given slightly later.

Finally, we summarize potential applications the present work can further deliver, as follows:

- In the area of nanoscale FETs (MOSFETs, FinFETs, etc.) modeling and simulation, this work suggests the inclusion of plasmons altered minority-carrier density in the highly doped source and drain region. We noticed that the literature simulation methods [3], [4] did not address the specific role of such minority-carrier density change as *additional numerical constraints* in the simulation. In other words, the simulated long-range effects on device characteristics as published in [3] and [4] might be overestimated. Thus, for the target FETs down to 5-nm node [14], such key constraints have to be incorporated to ensure accurate modeling and simulation.
- The discrepancies from semiconductor data in Fig. 4 may provide the opportunity to examine other many-body effects or to devise new and correct model. To show this, we take into account the hole-phonon interaction in the classical method. This is achieved by multiplying the right-hand side of (6) by a collision damping factor γ [3]: $\gamma = 1/\sqrt{1+1/(\omega_p \tau_m)^2}$, where τ_m is the momentum relaxation time, which can be obtained from the temperature and doping dependent mobility data published elsewhere [11]. Obviously, the classical model can produce a better agreement with data, as long as extra effects like hole-phonon interaction are included, as shown in Fig. 4. On the other hand, we found that even by incorporating all Coulomb interactions [15] (except the electron-hole one) in this work, the calculated temperature power law exponent using the quantum method (5) remains negative (not shown here). This suggests that a new and correct version of (5) should be derived *directly from the Hamiltonian* including Coulomb interactions [15], rather than the perturbation treatment [3].

IV. Conclusion

We have experimentally extracted potential fluctuations directly from the literature minority-carrier injection experiment. Plasmons as the origin of the extracted potential fluctuations have been identified. Potential applications have been drawn.

References

[1] D. Pines and D. Bohm, "A collective description of electron interactions: II. Collective vs individual particle aspects of the interactions," *Phys. Rev.*, vol. 85, no. 2, pp. 338–353, Jan. 1952.
[2] M. V. Fischetti *et al.*, "Theoretical study of some physical aspects of electronic transport in nMOSFETs at the 10-nm gate-length," *IEEE Trans. Electron Devices*, vol. 54, no. 9, pp. 2116–2136, Sep. 2007.
[3] M. V. Fischetti and S. E. Laux, "Long-range Coulomb interactions in small Si devices. Part I: Performance and reliability," *J. Appl. Phys.*, vol. 89, no. 2, pp. 1205–1231, Jan. 2001.
[4] K. Nakanishi, T. Uechi, and N. Sano, "Self-consistent Monte Carlo device simulations under nano-scale device structures: Role of Coulomb interaction, degeneracy, and boundary condition," in *Proc. IEDM*, Dec. 2009, pp. 79–82.
[5] M.-J. Chen *et al.*, "Probing long-range Coulomb interactions in nanoscale MOSFETs," *IEEE Electron Device Lett.*, vol. 34, no. 12, pp. 1563–1565, Dec. 2013.
[6] J. W. Slotboom and H. C. De Graaff, "Measurements of bandgap narrowing in Si bipolar transistors," *Solid-State Electron.*, vol. 19, no. 10, pp. 857–862, 1976.
[7] A. W. Wieder, "Arsenic emitter effects," in *Proc. IEDM*, 1978, pp. 460–462.
[8] D. D. Tang, "Heavy doping effects in p-n-p bipolar transistors," *IEEE Trans. Electron Devices*, vol. ED-27, no. 3, pp. 563–570, Mar. 1980.
[9] R. P. Mertens *et al.*, "Measurement of the minority-carrier transport parameters in heavily doped silicon," *IEEE Trans. Electron Devices*, vol. ED-27, no. 5, pp. 949–955, May 1980.
[10] S. E. Swirhun, D. E. Kane, and R. M. Swanson, "Temperature dependence of minority electron mobility and bandgap narrowing in p^+ Si," in *IEDM Tech. Dig.*, Dec. 1988, pp. 298–301.
[11] R. F. Pierret, *Advanced Semiconductor Fundamentals*. Reading, MA, USA: Addison-Wesley, 1987.
[12] M. S. Lundstrom, *Fundamentals of Carrier Transport*, 2nd ed. Cambridge, U.K.: Cambridge Univ. Press, 2000.
[13] M. J. Chen *et al.*, "Temperature-oriented mobility measurement and simulation to assess surface roughness in ultrathin-gate-oxide (≈1 nm) nMOSFETs and its TEM evidence," *IEEE Trans. Electron Devices*, vol. 59, no. 4, pp. 949–955, Apr. 2012.
[14] (2013). *International Technology Roadmap for Semiconductors (ITRS)* (ITRS 2013 Edition) [Online]. Available: http://www.itrs.net
[15] D. Pines, "A Collective description of electron interactions: IV. Electron interaction in metals," *Phys. Rev.*, vol. 92, no. 3, pp. 626–636, Nov. 1953.